sustainability

MDPI

Article

Study on Optimization Scheme of Slant Transition for Offshore Wind Turbine Foundation

Zhuye Huang [1], Yong Feng [1] and Zhenyu Wang [2,*]

[1] School of Civil Engineering and Architecture, Zhejiang University of Science and Technology, Hangzhou 310023, China; huangzhuye@zust.edu.cn (Z.H.); 15397091123@163.com (Y.F.)
[2] College of Civil Engineering and Architecture, Zhejiang University, Hangzhou 310058, China
* Correspondence: wzyu@zju.edu.cn

Abstract: Offshore wind power stands as a prime exemplar of high-end technological innovation in the renewable energy sector and is poised to be one of the high-growth industries of the future. In this study, a static mechanics and fatigue characteristic curve approach was utilized, employing both Abaqus and Fe-safe for the simulation analysis of the braced foundation transition sections in an offshore wind farm project in Shantou, Guangdong. The analysis revealed vulnerabilities in the stiffener plates and base plates of the transition sections. By increasing the thickness of the stiffener plates and adding sub-beams to the base plates, the structural stress was effectively reduced by 10–50%, thus ensuring the safety and suitability of the turbines. This provides a reference for the design of similar engineering transition sections.

Keywords: offshore wind turbine; slant supporting transition foundation; finite element analysis; structural optimization

check for updates

Citation: Huang, Z.; Feng, Y.; Wang, Z. Study on Optimization Scheme of Slant Transition for Offshore Wind Turbine Foundation. *Sustainability* **2024**, *16*, 5489. https://doi.org/10.3390/su16135489

Academic Editor: Firoz Alam

Received: 14 May 2024
Revised: 16 June 2024
Accepted: 24 June 2024
Published: 27 June 2024

Copyright: © 2024 by the authors. Licensee MDPI, Basel, Switzerland. This article is an open access article distributed under the terms and conditions of the Creative Commons Attribution (CC BY) license (https://creativecommons.org/licenses/by/4.0/).

1. Introduction

As the era progresses, both energy demands and environmental pressures are on the rise, drawing increasing attention to wind energy. Recognized as a natural, pollution-free renewable source, wind energy is distinguished for its efficient and clean power generation capabilities [1,2]. Furthermore, China is endowed with abundant offshore wind resources, characterized by an extensive coastline of about 18,000 km, primarily located in the economically prosperous and high-demand southeastern coastal areas, which are deficient in conventional energy sources. Recent resource surveys reveal that the exploitable wind energy reserves in China's nearshore areas amount to approximately 750 gigawatts, with the majority concentrated in the East China Sea, where wind speeds are higher and resources are more plentiful [3,4]. Consequently, offshore wind power has become a key focus in the development of renewable energy in China.

The basic structural forms of offshore wind turbine mainly include pile foundation, gravity foundation and Schemejacket foundation. The foundation of the jacket frame has advantages such as high stiffness and good safety, which is also suitable for shallow and deep water areas. So, it is currently widely used [5,6]. The foundation of the jacket mainly consists of the upper transition, the jacket in the middle and the pile (cylinder) foundation in the lower part. The upper transition needs to ensure that the wind turbine load is effectively transmitted to the lower duct supporting structure, playing a crucial role in connecting the upper and lower parts. Therefore, the design of the transition of the jacket foundation is mainly based on the strength of its own structure and the fatigue resistance ability, which is the key factor affecting the entire jacket foundation design [7].

The common types of jacket foundation transition are box girder type, slant supporting type, cone type and so on. In order to further improve the economic efficiency of offshore wind turbines, scholars have conducted comparative optimization studies on these foundations. Guo Xiaohui [8] compared slant supporting type and box girder type

transition jackets through SACS software. He proposed an improved flange type transition for the further type. With ultimate load, the flange type transition has lower structural stress and lighter weight compared to the others. Wang Haijun [9] proposed a type of offshore wind turbine inverted Y-shaped jacket foundation structure which can effectively transfer the upper load to the lower foundation structure and fully exerting the high bearing performance of the foundation. Chong Gao [10] optimized and designed four forms of jacket for comparison. It was found that adding horizontal bars at the bottom of the jacket can significantly optimize its structure. He Zhengxing [11] conducted a comparative analysis of the flat box girder transition and the inclined box girder transition using finite element software. He found that the flat box girder transition has greater stiffness than the inclined box girder transition and can withstand larger wind turbine loads, which has more advantages in the design of large capacity wind turbine foundations.

In addition, scholars analyze and study this field from the aspects of bearing capacity and fatigue. Liu Zhenhai [12] conducted numerical analysis on wind-induced fatigue of four pile jacket foundations. He found that the main load causing fatigue damage to the jacket foundation is the load with a number of cycles in the range of 5×10^4 to 5×10^7. Jiang Pengbin [13] used ANSYS to establish four sets of transition models and compared them. They found that setting shear keys in the transition can significantly improve the axial bearing capacity of the transition. Besides, The longer the transition length, the slightly increased bearing capacity. Song Ji [14] analyzed the transition with shear keys mainly subjected to bending loads and explained that the end of the transition bears a large radial force. He suggested that the shear keys should be set in the middle of the transition to reduce fatigue damage.

3 MW to 5 MW is popular in wind energy design. Lu Daohui [15] conducted a fatigue strength evaluation of the transition support structure of a 3 MW offshore wind turbine jacket under random wave loads. He found that the fatigue strength of the transition structure of the jacket foundation has a relatively small impact. Schaumann P [16] studied the fatigue problem in deep water through theoretical and numerical analysis. Numerical calculations show that there is a non-linear relationship between the size of shear keys and the stress concentration coefficient of the welding foot. Gradually increasing the number of shear keys will lead to a decrease and then an increase in the stress concentration phenomenon of the welding foot. Garbatov Y [17] used various fatigue damage calculation methods to analyze the fatigue life of a fixed 5 MW offshore wind turbine support structure, taking into account the influence of seawater corrosion on the fatigue life of the support structure. Tabeshpour [18] analyzed the fatigue damage of offshore wind turbine foundations under irregular first-order linear wave forces based on P-M wave spectrum, Airy's linear wave theory and Morrison's equation.

Taking the transition project of Guangdong Da Tang International Shantou Nan Ao Le Men I offshore wind farm project as an example, the paper conducts numerical simulation of the slant supporting transition scheme and proposes an optimization scheme to ensure construction quality, facilitate construction and reduce costs, which also provide a reference for the design of the transition of offshore wind turbine duct support foundation under similar conditions.

2. Establishment of Finite Element Model

Slant supporting transitions are mainly used in offshore wind farms such as Alpha Ventus (Germany), Beatrice (Scotland), Ormonde (Britain) and Thorton Bank (Belgium) [19]. According to the project prototype, the finite element analysis software ABAQUS is used to establish the finite element model with reference to the actual engineering parameters.

2.1. Finite Element Model Design

The model is mainly composed of main steel pipe, slant support plate, stiffening ring, supporting pipe, bottom plate and stiffening plate. The slant supporting transition is shown in Figure 1. The upper tower is connected to the main steel pipe through a flange at the

top position of the foundation ring. And the main steel pipe is connected to the main leg of the lower truss structure through the bottom plate. In order to effectively transfer the load and ensure the structural safety, the supported pipe extends upward from the connection position of each truss leg on the bottom plate and it is supported at the top of the foundation ring of the main steel pipe through the slant support pipe. At the same time, a stiffening ring is set at the connection position of the main steel pipe. The stiffening ring can increase the welding area between the main steel pipe and the slant support plate, on the other hand. It can effectively release the strain energy and avoid the stress concentration at the connection position of the foundation ring top.

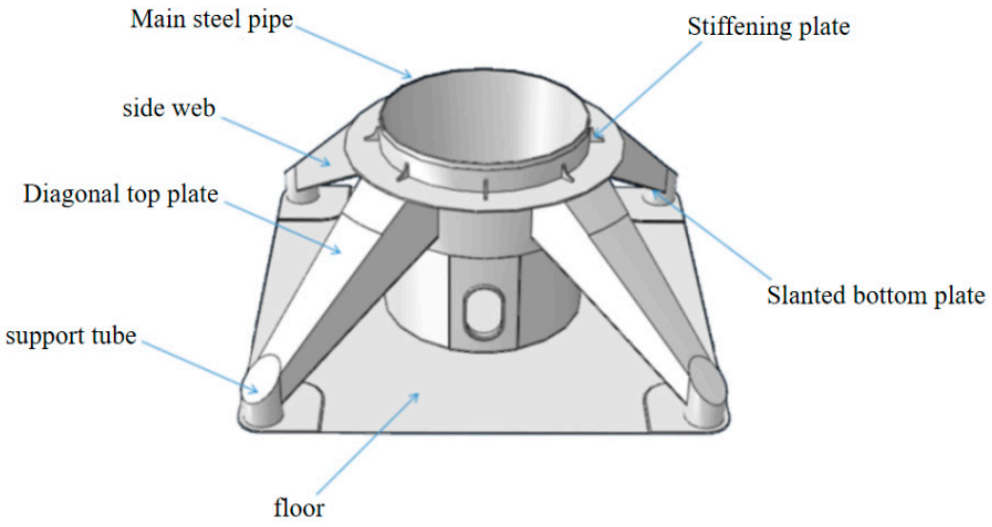


Figure 1. Schematic diagram of slant supporting transition.

2.2. Finite Element Model Parameter Settings

2.2.1. Selection of Unit Characteristics

When modeling the transition section of offshore wind turbine foundations, solid elements, beam elements and rod elements were mainly used. The entire transition section is made up of solid elements. The solid elements mainly adopt the quadratic tetrahedral element (C3D10), which can construct meshes of any shape. Due to the relative complexity of the model and the phenomenon of stress concentration in local areas, quadratic fully integrated elements (C3D20) are used for local analysis. This makes the stress calculation results more accurate and the analysis accuracy will not be significantly affected when the mesh is twisted or deformed. In general, the problem of shear self-locking will not occur. Besides, many slants supports in the jacket model under the transition section and the connection is more complex, beam elements and rod elements are used for modeling. Because the beam elements and rod elements can effectively simulate solid shapes such as angle steel combinations, rectangular steel and angle steel, which can ensure that the calculation results are closer to the real situation. In addition, this method can also enhance the visualization characteristics of the structure and incorporate the influencing factors of shear deformation.

2.2.2. Structural Material Parameters

The transition of the foundation of the jacket type offshore wind turbine is mainly composed of steel pipes with different diameters. Considering that the structure should meet the requirements and performance of use, the steel models used are mainly DH36 and EH36.

The constitutive relationship of materials is based on the selection of the widely used hardening elastic-plastic model for steel reinforcement. This model considers the stress-strain relationship of materials before the yield limit as linear elasticity, while after the

yield limit, the relationship exhibits linear strengthening characteristics. The model is more realistic and not as complex as the curve elastic-plastic strengthening model. The values of constitutive parameters for steel bars are mainly based on (GB/T50010-2010).

2.2.3. Load Arrangement

This article considers the load transmitted from the wind turbine tower to the top flange of the transition. Therefore, move up a certain distance along the center of the top surface of the transition to select a reference point (RP-1, Figure 2), and then couple the reference point with the top surface of the main steel pipe in the transition (Figure 2), loading both force and bending moment on this reference point (Figure 3).

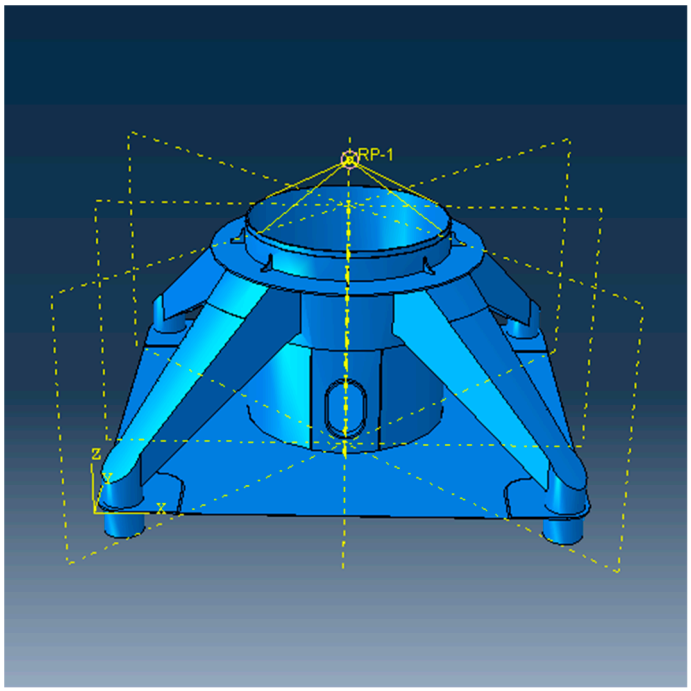


Figure 2. Load coupling arrangement.

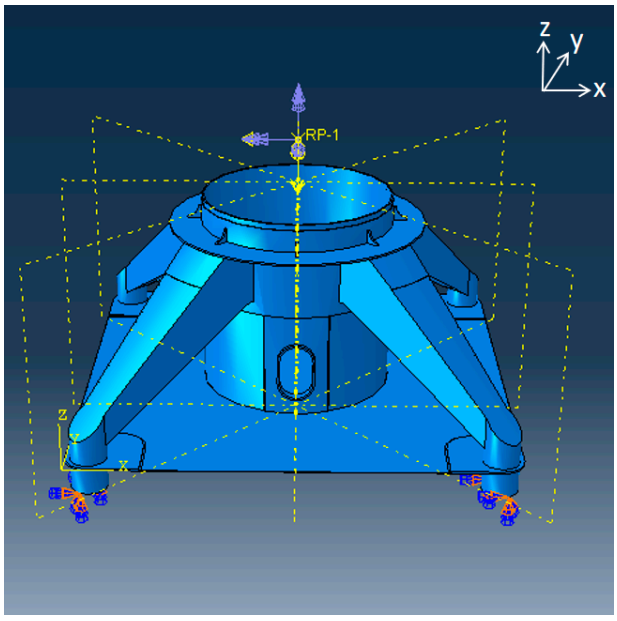


Figure 3. Load direction.

The finite model is a wind turbine foundation structure with four legs and a conduit frame. According to the Design Regulations for Wind Turbine Foundation [20,21], both the normal working state and ultimate state should be considered. According to the information provided by the design institute and the specification "Load and Site Conditions for Wind Turbines" (DNVGL-ST-0437) [22], the safety factor is set to 1.5. The two working condition loads are obtained as shown in Table 1.

Table 1. Working condition load.

Working Condition	Normal Condition	Extreme Conditions	Equivalent Fatigue
FX (kN)	1811.55	2622.9	127.4
FY (kN)	495.75	3912.75	292.6
FZ (kN)	1266.02	11,759.4	188.1
MX (kN·M)	50,230.4	288,759	4753.5
MY (kN·M)	118,090	138,104	14,083.6
MZ (kN·M)	13,217	28,433.3	22,577.3

2.2.4. Load and Constraints

Due to the fact that all components of the transition are connected by welding during the actual machining process modeling, tie binding interaction is adopted.

A conduit frame was designed below the four supporting pipes in the transition (Figure 4), and a fully fixed constraint was set on the bottom surface of the conduit frame. The support pipes on the top surface of the jacket and the bottom surface of the transition section adopt tie to ensure that there is no relative displacement during the simulation process. All slant support of the jacket use tie to form the four pillars of the jacket to avoid relative displacement. At the same time, all connectors of the central truss of the jacket are embedded in the angle steel parts of the four pillars of the jacket, without considering the bond slip between the two.

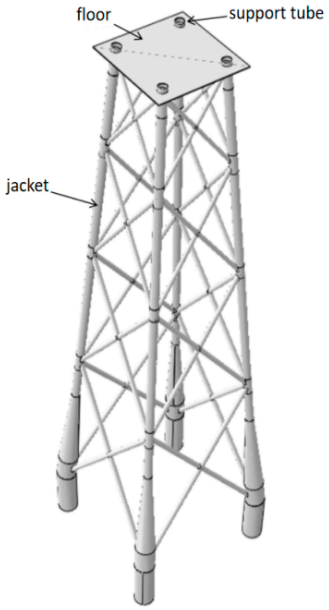


Figure 4. Conduit frame modeling.

3. Mechanics Analysis of the Transition of Offshore Wind Turbine Foundation

This study performed static analysis on the transition of the offshore wind turbine foundation, then calculated the strength of the structure to ensure that it meet the requirements. At the same time, the maximum stress value and position was identified on the structure. And the subsequent optimization results were compared and analyzed.

3.1. Statics Analysis of Transition

Through static analysis of the structure, the maximum stress values of the structure under two working conditions are obtained. The maximum stress under safe operating conditions is 194.5 MPa, and the maximum stress under extreme operating conditions is 384.1 MPa (Figures 5 and 6). The maximum stress of slant support transition section under normal and extreme working conditions are both at the position of stiffening plate. This may be because the composite structure at the lower part of the slant support transition section has large stiffness and strong constraint, so the stress on the lower part is relatively small; At the same time, the slant support transition section is only externally equipped with stiffened plates, and has a certain slope due to the inclined roof structure. Therefore, the upper part of the slant support transition section has no obvious constraint, so the upper stress is the largest.

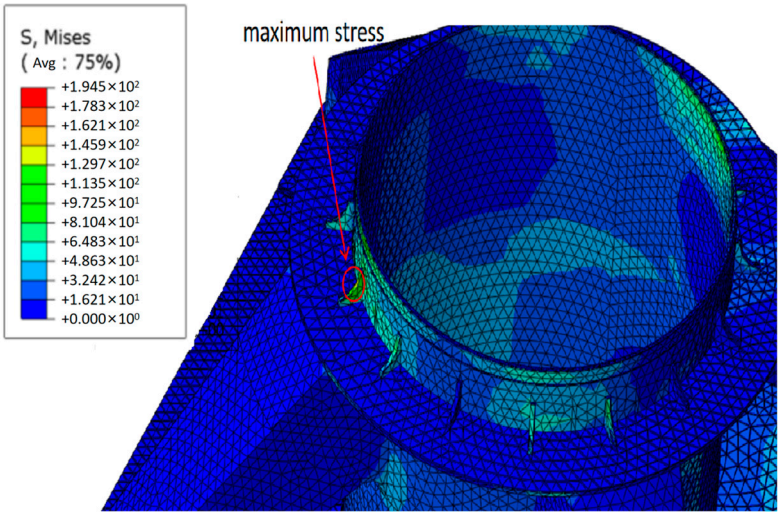


Figure 5. Normal working conditions.

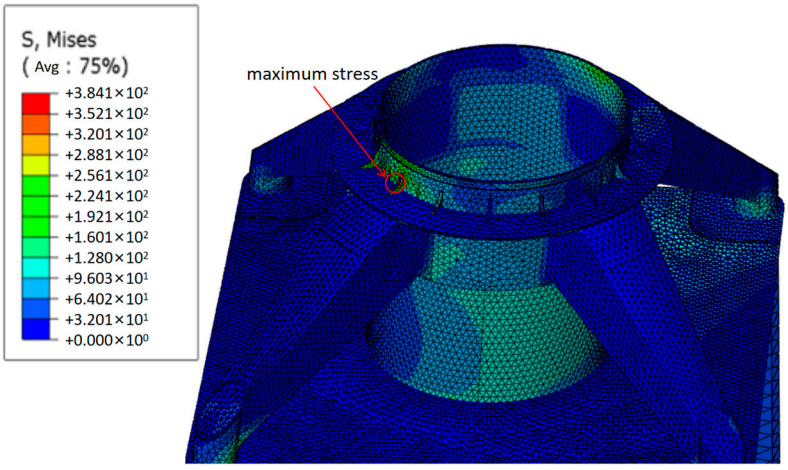


Figure 6. Extreme working conditions.

The maximum stress under extreme operating conditions increases by 97.5% relative to the maximum stress under safe operating conditions on the same point which is at the stiffener plate on the top edge of the main steel pipe in the transition. At the same time, the maximum stress at the stiffening plate under extreme working conditions exceeds the yield strength of the steel. This indicate that there are original design defects at the stiffening plate, so further optimization is needed.

In addition, under the two working conditions, the transition experiences the second highest stress at the bottom plate. The maximum stress experienced by the safety condition on the bottom plate is 122.5 MPa, and the maximum stress experienced by the ultimate condition on the bottom plate is 235.6 MPa. The maximum stress under the ultimate condition increased by 92.3% relative to the maximum stress under the safety condition.

When the load under normal working conditions acts on the structure, the maximum stress of the structure is much smaller than that under extreme working conditions. The maximum stress at the stiffening plate on the bottom plate and main steel pipe edge under extreme working conditions is nearly twice the maximum stress under normal working conditions. Therefore, deepening the design under extreme operating conditions is sufficient.

3.2. Transition Fatigue Analysis

The fatigue of the transition is mainly calculated and analyzed under normal working conditions through two methods: S-N curve and FE-SAFE2020 software. The given equivalent loads used in fatigue analysis are shown in Table 1.

3.2.1. S-N Curve

According to the fatigue analysis of offshore wind turbine foundation structures, the S-N curve is based on the DNV-RP-C203 specification formula:

$$\log N = \log \bar{a} - M \log(\Delta\sigma(\frac{t}{t_{ref}})^{k}) \quad (1)$$

In the formula: N is the number of cycles; $\triangle\sigma$ is the fatigue stress amplitude (MPa); M is the negative slope of the S-N curve; Log ā is the fatigue damage constant; t is the calculated point thickness; t_{ref} is the reference thickness calculated for thickness effect; K is the thickness index.

Where $\triangle\sigma$ = 7.51 MPa, m = 3, k = 0.15, log ā= 12.049, $\frac{t}{t_{ref}}$ = 1, based on the stress in the ultimate static cloud diagram, N = $10^{9.4}$ cycles was calculated. Mises stress under fatigue equivalent load is shown in Figure 7.

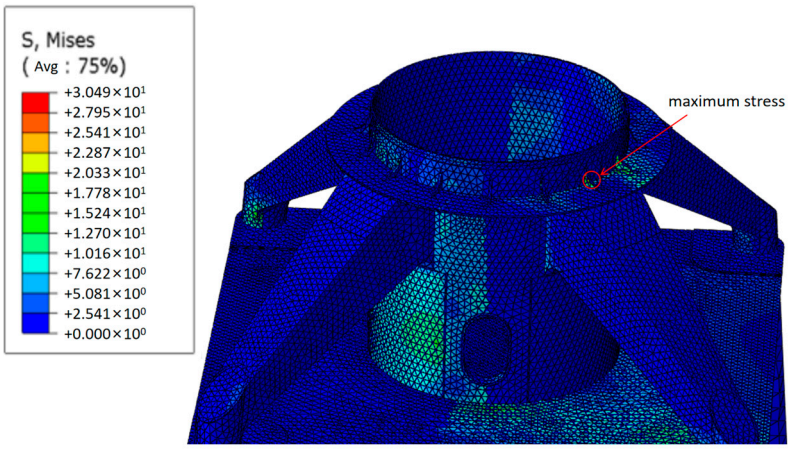


Figure 7. Stress under fatigue equivalent load.

3.2.2. FE-SAFE

Meanwhile, extreme condition load is discussed as a reference. The fatigue life cloud map is obtained by analyzing and calculating the static analysis results. The tensile strength of EH36 steel was estimated to be 490 MPa, with Ef′ = 0.59 and Sf ′ = 735 MPa, and the load spectrum was selected as symmetric cyclic. The minimum number of fatigue cycles that can be obtained is 10^{14} under the extreme condition, which occurs at the junction of the

reinforced plate and the main steel pipe. The local fatigue cycle cloud map is shown in Figure 8.

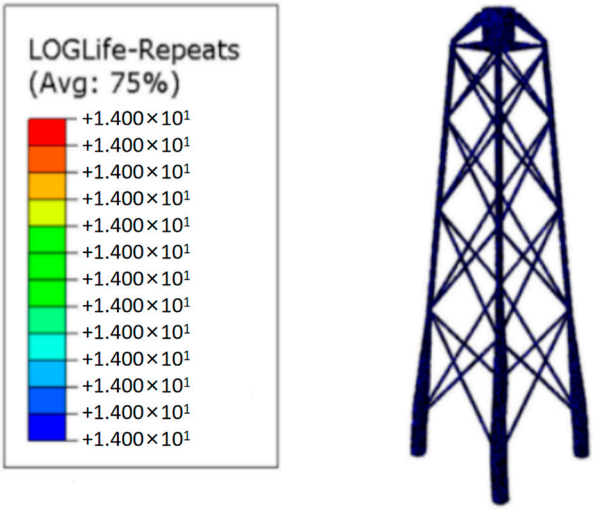


Figure 8. Fatigue cycle cloud map under extreme load.

N curve and FE-SAFE software were used to calculate and analyze the transition section under fatigue conditions. The S-N curve analysis shows that the number of fatigue cycles at the stiffening plate is the smallest. Therefore, when optimizing the structure in the future, priority can be given to optimizing from the stiffening plate; The total number of fatigue cycles calculated using FE-SAFE software is 10^{14}. This is because FE-SAFE uses the tensile strength of the material for calculation, resulting in a larger calculation range. At the same time, the fatigue load loaded on the transition section is too small compared to the tensile strength of the structural material, and the maximum number of FE-SAFE cycles is only 10^{14}. This means that the transition section theoretically has almost no fatigue damage. According to the requirements of the specification, the number of fatigue cycles should be more than 10^8, which is within a reasonable range. According to the S-N curve and FE-SAFE software, the calculation results of the slant support transition section under the fatigue condition are far greater than the design requirements, so it shows that the fatigue strength meets the use requirements. In addition, the fatigue cycle cloud map obtained through FE-SAFE software analysis clearly shows that the minimum fatigue cycle is located at the point of maximum stress, which is the middle position of the stiffening plate. Therefore, targeted optimization can be carried out in the future.

4. Optimization

From the stress analysis under extreme conditions in the previous text, it can be seen that the largest stress of the model at the stiffening plate is 384.1 MPa, which exceeds the yield strength of the steel and can easily lead to permanent deformation of the components. Therefore, it is necessary to thicken the stiffening plate on the strengthening ring first.

In addition, most parts in the model are subjected to stresses below 200 MPa. The maximum stress value of 235.6 MPa occurs on the bottom plate. The stress on the bottom plate in the range of 200–235.6 MPa accounts for approximately 0.08% of the entire bottom plate, which is tiny. Meanwhile, the bottom plate is a 15 mm thin steel plate with size of 15.6 m × 15.6 m, it is a large surface area but only four pipe supports at the bottom. Therefore, this part can be optimized in order to reduce the stress and extend its service life.

4.1. Optimization of Stiffeners

1. Optimization plan

Thicken the stiffening plate on the strengthening ring, increasing the thickness from 75 mm to 100 mm, 120 mm, and 150 mm respectively.

2. Optimization results

Through static analysis, the stress cloud map of the optimized structure was obtained. The maximum stresses corresponding to the thickness of the stiffening plate in the transition of 100 mm/120 mm/150 mm are 379.9 MPa/335.5 MPa/357.1 MPa. (Figure 9 is the stress cloud map of reinforced plate 120 mm). respectively. Compared with the non-thickened part, the stresses have decreased by 1.1%/12.7%/7.0%.

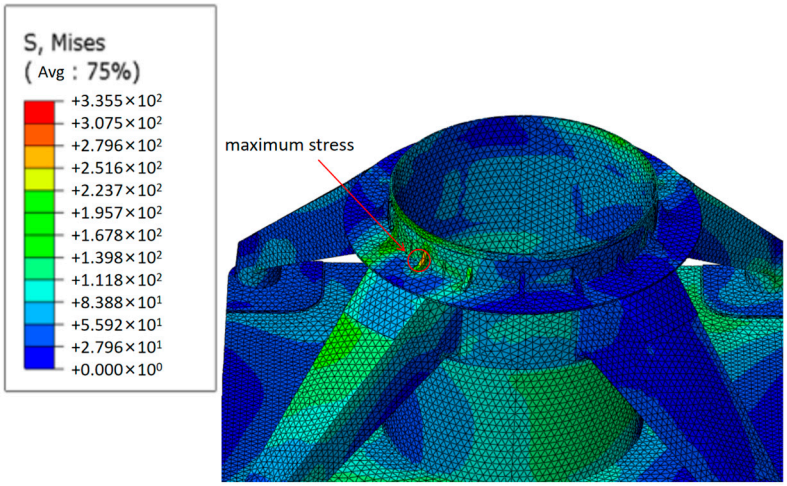


Figure 9. Stress cloud map of reinforced plate 120 mm.

As the thickness increases, the maximum stress in the transition first decreases and then increases. The transition represented by a thickness of 120 mm already meets the requirements for material yield strength. But from the stress cloud map, it can be seen that the position of the maximum stress in the transition is constantly changing with the thickness of the stiffening plate. The maximum stress gradually moves towards the edge of the stiffening plate near the main steel pipe as the thickness increases from the middle of the 75 mm thick stiffening plate, and then continuously moves downwards along the main steel pipe to the connection between the main steel pipe and the bottom plate. As a result, the maximum stress in the transition shows a trend of first decreasing and then increasing with the increase of the thickness of the stiffening plate. The stress corresponding to the middle part of the stiffened plate with a thickness of 100 mm/120 mm/150 mm is 359.1 MPa/333.9 MPa/309.1 MPa, respectively. Compared with the non-thickened part, the stress decreases by 6.5%/13.1%/19.5%. The stress at the stiffening plate decreases continuously with increasing thickness. Therefore, increasing the thickness of the stiffening plate can reduce the stress at the stiffening plate and gradually move the maximum stress towards the bottom plate, making subsequent bottom plate optimization more necessary.

3. Fatigue check

Perform fatigue stress analysis on a model with a stiffener plate thickness of 120 mm, and obtain a fatigue stress cloud map as Figure 10:

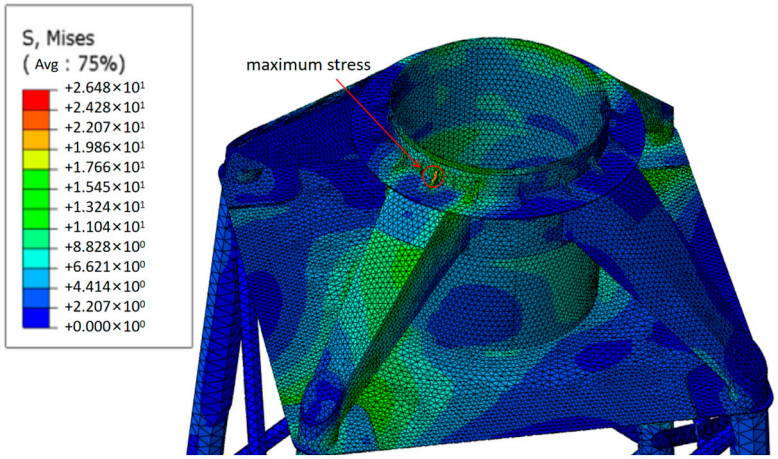


Figure 10. Fatigue cycle cloud map.

According to the stress in the fatigue static cloud map, the △σ at the stiffening plate is 7.25 MPa, and the △σ at the junction of the bottom plate and the thickened plate is 4.53 MPa. Therefore, $N_1 = 10^{9.46}$, $N_2 = 10^{10.08}$. So the fatigue strength of the structure also meets the requirements. Under the action of fatigue loads, the hot spot stress of the structure decreases, indicating that the damage value of the structure also decreases and the fatigue life of the structure also increases.

4.2. Bottom Plate Optimization

1. Optimization plan

Due to the high stress on the bottom plate, it is considered to add an assistant beam below the bottom plate as an optimization solution. The assistant beam is made of H-shaped steel with material DH36 of grade 10. The arrangement of assistant beams can be divided into two types:

The first method is to evenly arrange the auxiliary beams under the bottom plate. Under the entire bottom plate, evenly divide the bottom plate into 8 equal parts using an axis, and arrange the secondary beams horizontally and vertically according to the position of the axis. The spacing between each axis is 1950 mm.

The second method is mainly to arrange assistant beams at the locations below the bottom plate where the stress is relatively high based on the stress cloud map under extreme working conditions. A total of 12 assistant beams are arranged horizontally and vertically on the entire bottom plate. According to the stress cloud map under extreme working conditions, the maximum stress on the bottom plate occurs at the junction of the thickened plate and the bottom plate. So, four secondary beams are concentrated below the thickened plate position and displaced 750 mm towards the edge, that is, another secondary beam is arranged at three-quarters of the thickened plate (which is also the bottom of the outer edge of the support pipe), and finally a secondary beam is arranged below the outer edge of the main steel pipe, and then arranged symmetrically on both sides. The specific layout positions are shown in Figures 11 and 12.

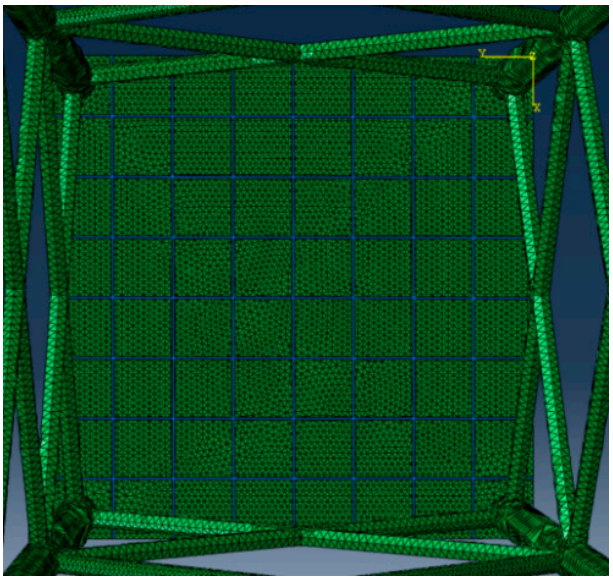


Figure 11. Assistant beam layout method one.

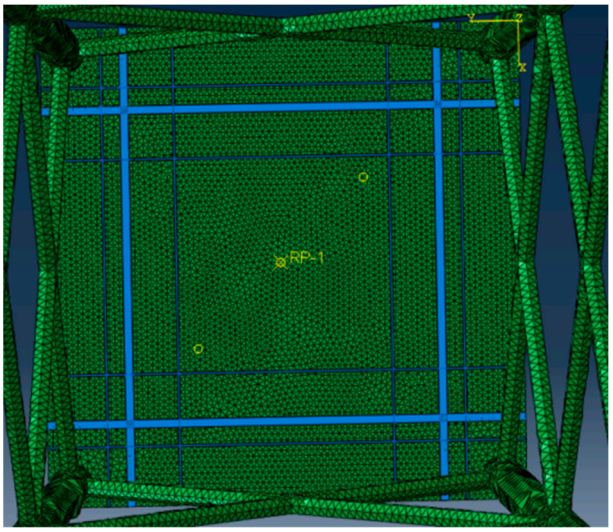


Figure 12. Assistant beam layout method two.

2. Optimization results

Through static analysis, the stress cloud map of the optimized structure was obtained. The stress on the upper and lower bottom plates decreased to 228.9 MPa, while the stress on the upper surface of bottom plate decreased significantly, and the stress on the lower surface also decreased relatively. At the same time, the maximum stress position shifted towards the edge. The maximum stress on the upper surface is 115.6 MPa, and the maximum stress on the lower surface is 206.8 MPa. Compared to the maximum stress on the upper surface of the bottom plate before optimization, which was 235.6 MPa, the maximum stress in scheme one decreased by 2.9%, and the maximum stress on the upper surface of scheme two decreased by 50.9%; The maximum stress on the lower surface before optimization was 232.9 MPa, while the maximum stress in scheme one decreased by 1.7%. The maximum stress on the lower surface in scheme two shifted 760 mm outward, a decrease of 11.2%.

According to the comparison of stress before and after optimization, adding a secondary beam can slightly reduce the maximum stress of the transition section model and significantly reduce the stress on the upper and lower surfaces of the bottom plate. Because the secondary beam is arranged below the bottom plate, it increases the constraint effect

of the bottom plate below the model but the constraint effect above the transition section is not significant. However, the maximum stress of the slant support transition section model is above the model, so increasing the secondary beam will reduce the stress amplitude of the upper and lower surfaces of the bottom plate more than reducing the overall stress of the model. In addition, the maximum stress reduction amplitude on the upper surface is greater than that on the lower surface in both schemes, but the displacement trend at the super edge of the lower surface is more pronounced than that on the upper surface. Meanwhile, compared with Scheme one, Scheme two has a more significant effect on reducing the stress on the bottom plate. Because arranging secondary beams in areas with concentrated stress can more effectively reduce the maximum stress at that location and bring the maximum stress closer to the edge. Uniformly arranging secondary beams uniformly increases the constraint effect on the entire bottom plate, so the optimization effect is not significant compared to Scheme two.

3. Fatigue check

A fatigue stress analysis will be conducted on the model of secondary beams concentrated at the point of maximum stress on the bottom plate, and the fatigue stress cloud map obtained is as follows:

According to the stress in the fatigue static cloud map, the $\triangle\sigma$ at the stiffening plate is 6.93 MPa, and the $\triangle\sigma$ at the junction of the bottom plate and the thickened plate is 4.19 MPa. Therefore, $N_1 = 10^{9.52}$, $N_2 = 10^{10.17}$. The fatigue strength of the structure meets the requirements. According to the comparison of fatigue results before optimization (Figure 7) and after optimization (Figure 13), the fatigue damage degree of the structure on the bottom plate has been reduced, and the fatigue life has been significantly improved.

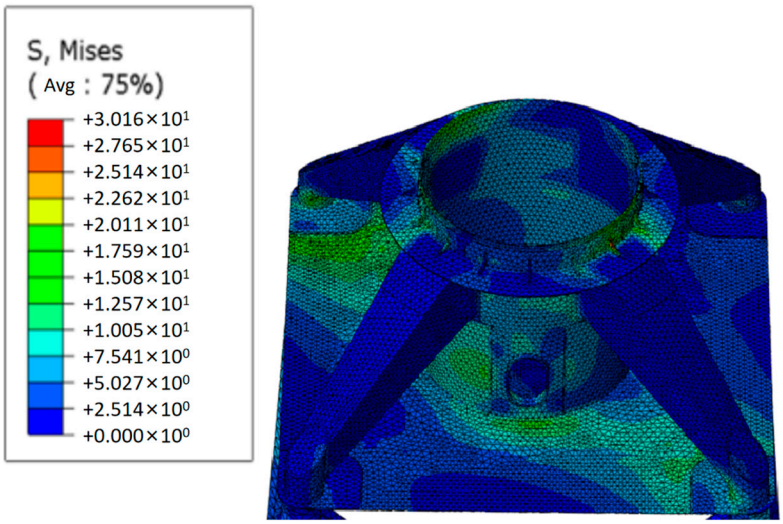


Figure 13. Stress distribution under equivalent fatigue load.

5. Conclusions

Based on the project of slant supporting transition in the wind turbine foundation design of an offshore wind farm project in Shantou, Guangdong, this paper uses static analysis to study the strength and fatigue life, so as to further optimize its design. After analysis and discussion, the main conclusions are as follows:

1. The stress of the slant supporting transition model is transferred to the jacket and bottom plate below through the main steel pipe—stiffening plate—stiffening ring—inclined plate—support pipe along the load direction. The maximum stress occurs in the middle of the stiffened plate, followed by the second maximum stress at the edge of thick plate of the bottom.
2. Increasing the thickness of the stiffening plate from 75 mm to 150 mm, the stress on the transition plate first decreases and then increases, and the maximum stress position

moves towards the bottom plate. When the thickness is increased to 120 mm, the maximum stress in the transition is less than the yield strength of the steel. The stress on the stiffening plate decreases by 12.7%, and the fatigue cycle increases by 128.3%. Therefore, when considering the amount of steel which is used on the transition part, stress can be reduced by appropriately increasing the thickness of the stiffening plate.

3. Placing assistant beams at the maximum stress point below the bottom plate resulted in a 50.9% decrease in stress on the upper surface of the bottom plate and an 11.2% decrease in stress on the lower surface. At the same time, the maximum stress position moved towards the edge, resulting in a more significant effect than uniformly placing assistant beams below the bottom plate. Therefore, when considering the amount of steel, the spacing between assistant beams can be adjusted to effectively reduce the stress on the bottom plate.

Based on the analysis of engineering examples and structural models, this paper proposes an optimization scheme for the slant supporting transition to ensure the construction quality and facilitate the construction of the project, which can provide a reference for the design of the transition of offshore wind turbine pipe rack foundation under similar conditions. At the same time, the optimization scheme is relatively one-sided and thin, which is only applicable to slant support transition sections, rather than all jacket transition sections. The optimization plan is only effective in reducing stress and ensuring structural stability, but does not consider reducing the weight of the structure or reducing construction difficulty. Because in the future, we will conduct the following work as further research:

1. Consider the influence of more factors on the stress distribution of slant support transition section, such as slant support angle, main cylinder height, etc.
2. Conduct relevant practical engineering experiments on the model, and compare and verify the experimental data with simulation data.
3. Consider the optimization simulation of slant support transition section in terms of reducing structural weight, reducing construction difficulty and other aspects.

Author Contributions: Conceptualization, Z.H. and Y.F.; methodology, Z.H.; software and analysis, Y.F.; writing-original draft preparation, Z.H. and Y.F.; writing—review and editing, Z.H.; supervision, Z.W. All authors have read and agreed to the published version of the manuscript.

Funding: This research received no external funding.

Institutional Review Board Statement: Not applicable.

Informed Consent Statement: Not applicable.

Data Availability Statement: The data presented in this study are available on request from the corresponding author. The data are not publicly available for confidentiality reasons.

Conflicts of Interest: The authors declare no conflict of interest.

References

1. Guo, J.; Wang, H.; Luo, G. Numerical Analysis of Horizontal Bearing Capacity of Variable Diameter Pile Foundation for Offshore Wind tubine. *Sci. Technol. Eng.* **2022**, *22*, 3658–3664.
2. Zou, C.; Zhao, Q.; Zhang, G.; Xiong, B. Engineering Revolution: From a fossil energy era to a new energy era. *Nat. Gas Ind.* **2016**, *36*, 1–10.
3. Li, Z.; Song, L.; Ma, H. Research Progress of Offshore Wind Energy Resources Observation and Evaluation. *Adv. Earth Sci.* **2016**, *31*, 800–810.
4. Lan, Z. Preliminary Evaluation on the Geographic Distribution of Wind Energy Resources and Its Development and Utilization in China. Master's Thesis, Lanzhou University, Lanzhou, China, 2015.
5. Huang, W.; Liu, J.; Zhao, Z. The state of the art of study on offshore wind turbine structures and its development. *Ocean. Eng.* **2009**, *27*, 583–590.
6. Huang, Z. Comparison of technical routes for the development of offshore wind turbine models. *Chin. Foreign Energy* **2019**, *24*, 29–35.
7. Lian, J.; Liu, H.; Chen, Z. Research on the Mechanical Behavior of Truss-Type Supporting Structures for Wind Turbine. *Ind. Constr.* **2015**, *45*, 160–165.

8. Guo, X.; Wu, Z. Numerical Analysis of Jacket Transition. *China Offshore Planform* **2020**, *35*, 57–63.
9. Wang, H.; Tang, B.; Lian, J. Research on for force Characteristics of Offshore wind turbine Inverted Y-shaped Jacket Bucket Foundation. *Ocean. Eng.* **2022**, *40*, 112–120.
10. Gao, C. Optimization of offshore wind turbine multi-pile jacket type foundation jacket. *Technol. Style* **2017**, *1*, 128–129.
11. He, Z. Finite element analysis of offshore wind turbine jacket foundation transition based on ABAQUS. *Fujian Hydropower* **2021**, *1*, 65–69.
12. Liu, Z.; Chen, J.; Li, G. Numerical Analysis of Wind Induced Fatigue Based on Four-Pile. *Electr. Power Surv. Des.* **2023**, *3*, 51–56.
13. Pengbin, J. Study of Several Problem of Offshore Farm Wind Tube Foundation Design. Master's Thesis, Dalian University of Technology, Dalian, China, 2013.
14. Song, C. Connection of Offshore Wind Turbine' Tower and Base. *Shanxi Energy Conserv.* **2010**, *2*, 46–49.
15. Lu, D.; Yang, Y.; Huang, D. Offshore Wind Turbine under Random Wave Load Fatigue Strength Analysis of Foundation Key Structures. *Wind Energy Technol.* **2016**, *08*, 54–56.
16. Schaumann, P.; Lochte-Holtgreven, S.; Bechtel, A. Fatigue Design for Axially Loaded Grouted Connections of Offshore Wind Turbine Support Structures in Deeper Waters. In *Earth and Space 2010: Engineering, Science, Construction, and Operations in Challenging Environments*; American Society of Civil Engineers: Reston, VA, USA, 2010.
17. Garbatov, Y.; Yeter, B.; Guedes Soares, C. Fatigue damage analysis of a fixed offshore wind turbine supporting structure. *Dev. Marit. Transp. Exploit. Sea Resour.* **2014**, *29*, 415–424.
18. Tabeshpour, M.R.; Golafshani, A.A.; Seif, M.S. Comprehensive study on the results of tension leg platform responses in random sea. *J. Zhejiang Univ.-Sci. A* **2006**, *7*, 1305–1317. [CrossRef]
19. Pan, Z.; Wu, G.; Zhao, S. Topology Optimization Method for Transition Pieces of Offshore Jacket Wind Turbine Foundations. *China Offshore Platf.* **2019**, *34*, 6–13.
20. *DNV-RP-C203*; Fatigue Design of Offshore Steel Structures. DNV: Bærum, Norway, 2016.
21. *NB/T 10105-2018*; Code for Design of Wind Turbine Foundations of Offshore Wind Power Projects. National Energy Administration: Beijing, China, 2018.
22. *DNVGL-ST-0437*; Loads and Site Conditions for Wind Turbines. DNV: Bærum, Norway, 2016.

Disclaimer/Publisher's Note: The statements, opinions and data contained in all publications are solely those of the individual author(s) and contributor(s) and not of MDPI and/or the editor(s). MDPI and/or the editor(s) disclaim responsibility for any injury to people or property resulting from any ideas, methods, instructions or products referred to in the content.